Materials Science-Poland, 30(3), 2012, pp. 189-196
http://www.materialsscience.pwr.wroc.pl/
DOI: 10.2478/s13536-012-0022-3

VERSITA

TiO_2/bone composite materials for the separation of heavy metal impurities from waste water solutions

G. DAKROURY, SH. LABIB*, F.H. ABOU EL-NOUR

Nuclear Chemistry Department, Hot Laboratories Center, Atomic Energy Authority, P.O. box 13759 Cairo, Egypt.

Pure bone material obtained from cow meat, as apatite-rich material, and TiO_2-bone composite materials are prepared and studied to be used for heavy metal ions separation from waste water solutions. Meat wastes are chemically and thermally treated to control their microstructure in order to prepare the composite materials that fulfill all the requirements to be used as selective membranes with high performance, stability and mechanical strength. The prepared materials are analyzed using Hg-porosimetry for surface characterization, energy dispersive X-ray spectroscopy (EDAX) for elemental analysis and Fourier transform infrared spectroscopy (FTIR) for chemical composition investigation. Structural studies are performed using X-ray diffraction (XRD). Microstructural properties are studied using scanning electron microscopy (SEM) and specific surface area studies are performed using Brunauer-Emmet-Teller (BET) method. XRD studies show that multiphase structures are obtained as a result of 1h sintering at 700–1200 °C for both pure bone and TiO_2-bone composite materials. The factors affecting the transport of different heavy metal ions through the selected membranes are determined from permeation flux measurements. It is found that membrane pore size, membrane surface roughness and membrane surface charge are the key parameters that control the transport or rejection of heavy metal ions through the selected membranes.

Keywords: *meat bones, composite membranes, heavy metal ions, permeation flux, selectivity*

1. Introduction

Hazardous wastes may account for approximately 2–20 percent of all the wastes in the world. One of the most important categories of the wastes are heavy metal ions [1]. The dangerous effect of heavy metal ions results from their mobility in the liquid phase of the eco-system and their toxicity to the environment, even at low concentrations [2].

Hence, the treatment and the removal of heavy metal ions receive considerable attention [3]. There is an increasing interest in the application of materials of biological origin in heavy metal ions removal from aqueous solutions [4]. Waste utilization is necessary not only because of waste materials re-accumulating but also because natural raw materials are being exhausted and it will be great to reuse them [5]. In addition, there is an even growing need to develop clean, non-toxic, environmentally friendly green procedures [5] for porous material synthesis. So, the use of cow meat bones (meat wastes) is of a particular concern; these residues are considered as apatite-rich materials, mainly calcium hydroxyapatite (HAP, ($Ca_{10}(PO_4)_6(OH)_2$), and are used as low cost substitutes of hydroxyapatite in the removal of heavy metal ions [4].

Hydroxyapatite suffers from its brittleness and relatively poor mechanical properties [6]. Therefore, titania particles are added to improve the mechanical properties of the materials.

In this paper, an attempt is made to develop HAP and other calcium phosphates from natural and cheap wastes [7, 8] to prepare the composite materials that fulfill all the requirements to be used as selective membranes with high permeability, stability and mechanical strength [9] to separate heavy metal ions from waste water solutions.

2. Material and methods

2.1. Material preparation

Cow meat bones (meat wastes) are washed with water several times then dried at 60 °C for 72 h and 100 °C for 24 h. The dried bones are ground

*E-mail: dr_sh_labib@yahoo.com

Table 1. Composition and abbreviation of the samples.

Sample	Composition	Sintering temperature °C/1 h		
		700	900	1200
		Abbreviation		
Pure Bone	100 %	B7	B9	B12
Bone-Titania	50 %–50 %	BT7	BT9	BT12

for 2 h using an electrical mortar then sieved to 150 µm using an electrical siever (analysette siever, Germany). 10 g of each ground powder is aged in 250 ml 1 M HCl (Merck) and 1 M NaOH (Sigma Aldrich) and kept for 48 h, then washed several times with de-ionized water and dried at 100 °C for 48 h. The selected powder is divided into two parts: pure bone powder (B) and (bone-TiO_2) composite powder (BT), where bone and TiO_2 are mixed in the stoichiometric ratio (1:1) respectively.

The powders are mixed in isopropyl alcohol (99.5 %, Scharlau, Spain) to make homogeneous mixtures. All the used reagents are of A.R. grade. The pure and composite mixtures are dried at 100 °C for 48 h and thermally treated at 200 °C for 1 h at a heating rate of 10 °C/min. The powders are ground (using a mortar and a pestle) for 45 min, pressed uniaxially at 20 kN and calcined at 500 °C for 1 h at a heating rate of 10 °C/min. The green compacts are sintered at 700, 900 and 1200 °C for 1 h at a heating rate of 10 °C/min. The composition and abbreviation of the different samples are shown in Table 1.

2.2. Material characterization

Surface characteristics of the powders treated with acidic and basic media are studied using Hg-porosimetry (Micromeritics 9320, USA). The elemental analysis is performed using energy dispersive X-ray spectroscopy (EDAX) (Oxford 7322) with the system resolution of 127 eV and accelerating voltage of 25 kV. Fourier transform infrared spectroscopy (FTIR) analysis (Bomin, Canada) is carried out using KBr, where the spectra of the studied powders are obtained in the region of 500–4000 cm^{-1} with a resolution of 4 cm^{-1} at 1 scan/min. Phase identification is done using X-ray diffraction (XRD) (Philips Xpert multi purpose diffractometer), where the used X-ray tube is a copper tube operating at a voltage of 40 kV and a current of 30 mA. The samples are scanned at diffraction angles of 2θ (20–60°) at room temperature. The different phases are identified using Joint Committee on Powder Diffraction Standards (JCPDS) card numbers. Scanning electron microscopy (SEM) is employed for morphological studies using low vacuum scanning electron microscopy (JEOL 5600 LV, Japan). Specific surface areas of different samples are measured using Brunauer-Emmet-Teller (BET) method (Nova 3200 Series, USA).

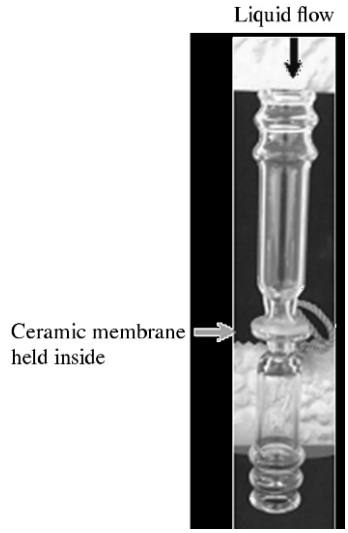

Fig. 1. Cross flow tubular filtration apparatus used in the separation experiments.

2.3. Performance studies

The suitable materials are selected for the separation of the ions of selected heavy metals (Cd, Fe and Cr). Heavy metal ions are obtained from cadmium nitrate (99 %, Merck, Germany), ferric nitrate (98 %, Alpha Chemika, India) and potassium dichromate (99.5 % Adwic, Egypt), respectively. The pH of the prepared solutions (50 ppm) is maintained at 3.

The separation experiments are conducted at room temperature under atmospheric pressure with a home-made cross flow tubular filtration apparatus, made from glass, where the appropriate membranes are sealed using elastomer O-ring and placed inside. The cross flow tubular filtration apparatus is adjusted in the vertical position, where the membranes can be held inside its inner diameter as marked by

Table 2. Surface characteristics of bone powders treated with acidic and basic media.

Sample	Total pore area (m^2/g)	Average pore diameter [nm]	Bulk density [g/c·c]	Apparent density [g/cc]	Porosity [vol.%]
B/acid	26.25	25	1.15	1.4	18.99
B/base	70.42	17.7	1.23	1.9	36.12

the grey arrow shown in Fig. 1. After each run, the membranes are washed several times with isopropyl alcohol.

The flux J of the different heavy metal ions through the membranes is determined using the following equation:

$$J = V/A \cdot \Delta t \quad (1)$$

where V is the permeate volume [L], A is the membrane area [m^2] and Δt is the permeation time [hour] [10].

Selectivity coefficient S is defined as the ratio of initial flux of heavy metal ion 1 and heavy metal ion 2, respectively [11].

$$S = J_{M1}/J_{M2} \quad (2)$$

3. Results and discussion

3.1. Hg-Porosimetry studies

To get powder with more porous structure, the powder dried at 100 °C for 24 h is aged in both acidic and basic media.

Hg-Porosimetry results show that the obtained powders are characterized by the presence of mesoporous structure (pores with internal width between 2–50 nm) [12], as shown in Table 2. The powder aged in the basic media is characterized by higher total pore area, lower average pore diameter and higher porosity [vol.%]. It means that the ageing in NaOH results in an increase in surface activity and the development of more porous structure, leading to a better surface structure.

3.2. Energy dispersive X-ray spectroscopy (EDAX) analysis

Elemental compositions of the powders, treated with basic media and then thermally treated at 200 °C for 1 h, are listed in Table 3; the main elements contained in the powders include O (47.5 %), Ca (33.9 %) and P (15.8 %), which represent the main constituents of apatite material. The Ca:P ratio of the present meat bones is found to be slightly calcium deficient [13]. The main natural pollutants contained in the bones are Na (1.58 %), Mg (0.62 %), Al (0.24 %) and Cl (0.14 %). No heavy metal pollutants are observed.

Table 3. Elemental analysis of bone powders thermally treated at 200 °C for 1 h.

Element	Percentage %
O	47.57
Ca	33.98
P	15.87
Na	01.58
Mg	00.62
Al	00.24
Cl	00.14

So, the elemental analysis suggests good quality of the ceramics derived from the meat bone as a mineral resource [13].

3.3. Fourier transform infrared spectroscopy (FTIR) analysis

FTIR spectra of B and BT powders thermally treated at 200 °C for 1 h are shown in Fig. 2. Beside the broad absorption band at 3396 cm^{-1} in B sample which can be assigned to O–H vibration band, both samples show the bands at (2900, 2861 cm^{-1}) corresponding to C–H bands, which can be referred to the presence of collagen and organic tissue [14]. The major hydroxyapatite characteristic bands at 1024 and 1028 cm^{-1} (P–O stretch band) are also present. Carbonate bands can be observed at 1410 and 1411 cm^{-1} since all the biological apatites belong to carbonated apatites [14]. The O–H bands, corresponding to strongly adsorbed H_2O, are ob-

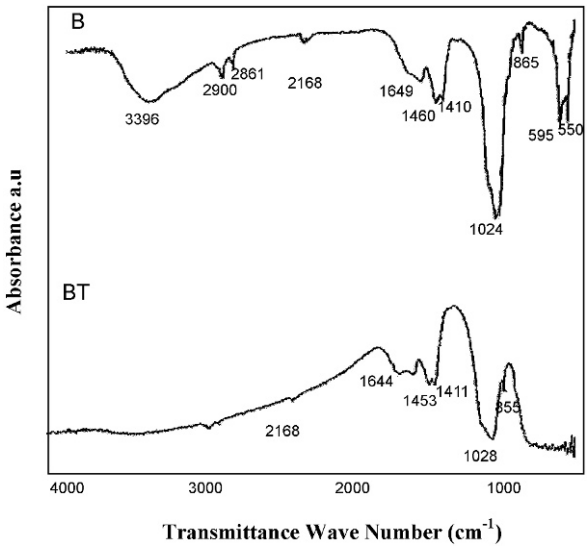

Fig. 2. FTIR spectra for B and BT powders thermally treated at 200 °C for 1 h.

served at 1649 and 1644 cm^{-1}; the bands observed at 865 and 855 cm^{-1} can be related to HAP nucleation. The B sample shows additional bands at 595, 550 cm^{-1} that also belong to P–O stretch and bending vibrations. Many authors report that the dominating peaks of TiO_2 (anatase) powders are centered at 400–430 cm^{-1} [15], however, these peaks are not observed here in the BT spectrum.

3.4. X-Ray diffraction (XRD) analysis

The performance or efficiency of a membrane is determined by two parameters: its selectivity and its permeation flux [16]. Therefore, a modification of membrane material by thermal treatment is done to make a complete study of different factors affecting the transport of heavy metal ions through the selected membranes [17]. Multiphase structures developed in different processing temperatures are studied using XRD.

The XRD results of B and BT compacts, thermally treated at 700, 900 and 1200 °C for 1 h, are given in Fig. 3(a–b) respectively. B compacts, thermally treated at the temperatures ranging from 700 to 1200 °C, are mainly composed of HAP phase that matches the JCPDS 74-0565 card number belonging to the hexagonal space group $P6_3/m$ (HAP). In addition, tri-calcium phosphate (TCP), $Ca_3(PO_4)_2$, is detected as a minor phase, and compared with (JCPDS-03-0713), belonging to rhombohedral space group R3C (β-TCP). The presence of TCP indicates the partial decomposition of HAP to TCP [7]. So, under heat treatment (700–1200 °C), the bones transform into well crystallized HAP and minor TCP phases [13]. In general, TCP phase is amorphous at the temperature range of 40–600 °C, and crystalline at higher temperatures [17].

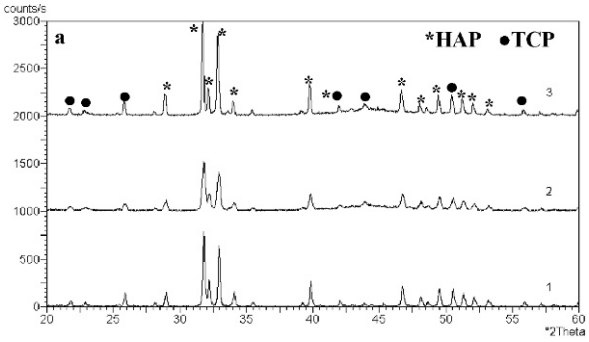

(a)

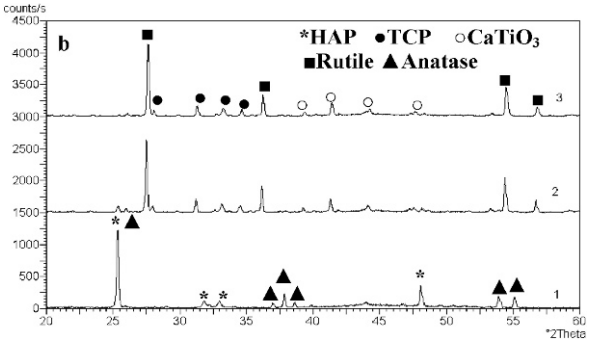

(b)

Fig. 3. XRD patterns of B compact membranes thermally treated for 1 h at (1) 700 °C (2) 900 °C and (3) 1200 °C.

The reflections of BT compacts are compared with HAP (JCPDS 74-0565), β-TCP (JCPDS 03-0713), orthorhombic space group Pbnm/62 ($CaTiO_3$) (JCPDS 78-1013), tetragonal space group (141) anatase (JCPDS 78-2486) and tetragonal space group $P4_2/mm$ (136) rutile (JCPDS 84-1283). As shown in Fig. 3(b), the only phases occurring at low temperatures are HAP and anatase but they disappear with increasing the temperature to 900 and 1200 °C. The new developed phases of rutile, β-TCP and $CaTiO_3$ are obtained at higher tempe-

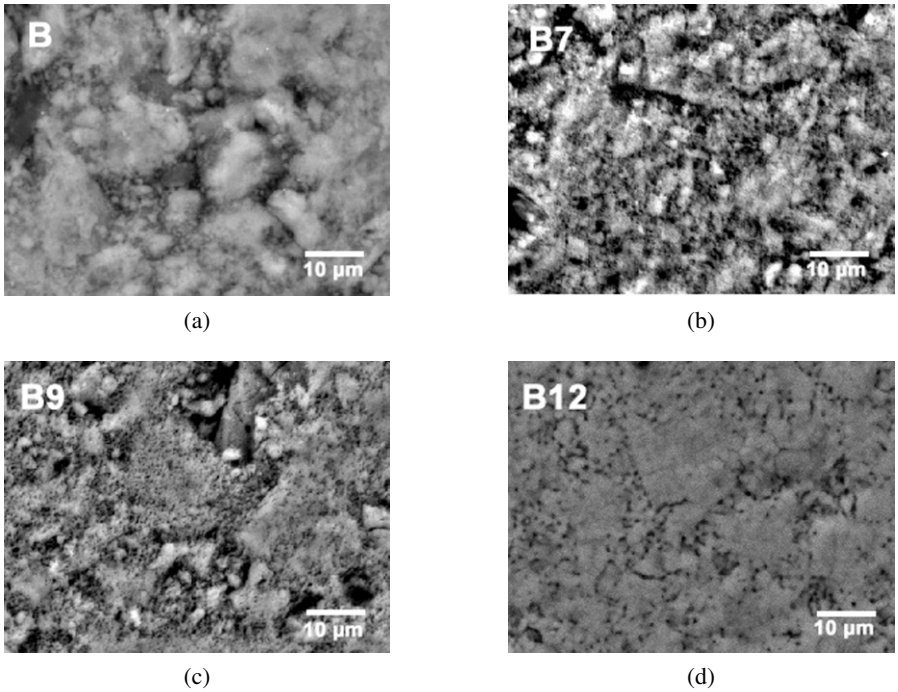

Fig. 4. SEM micrographs (magnification x = 1500) of B compacts thermally treated at (a) 200, (b) 700, (c) 900 and (d) 1200 °C.

ratures. These results confirm that titania interacts with HAP forming $Ca_3(PO_4)_2$ and $CaTiO_3$ [18].

3.5. Scanning electron microscopy (SEM) studies

SEM micrographs of B compacts are given in Fig. 4(a–d). B compacts, thermally treated at 200 °C for 1 h, consist of large particles of biologically mineralized hydroxyapatite with very low crystallinity, as shown in Fig. 4(a) [13]. As the result of thermal treatment at the temperature range of 700–1200 °C for 1 h, the bones transform into well-crystallized (HAP-TCP) composite crystals [13]. Porous and rough structures are obtained at the temperature range of 700–900 °C, Fig. 4(b–c). At 1200 °C, porous HAP and densified TCP phases, having smooth texture, are distributed homogeneously, Fig. 4(d). The porous HAP structure consists of hexagonal arrays with spherical pores. On the other hand, TCP structure consists of densified oval particles.

The addition of TiO_2 to the bone material improves the microstructure, as shown in Fig. 5(a–c), which can be related to the interaction of TiO_2 with HAP as outlined before [18]. The porous skeletal structure obtained at 700 °C, Fig. 5(a), transforms into the very fine composite microstructure with tiny oval and hexagonal crystallites after increasing the temperature to 900 °C, Fig. 5(b). At 1200 °C, multiphase structures of porous $CaTiO_3$, tetragonal rutile and embedded densified area of oval β-TCP particles are developed, Fig. 5(c). As shown, the multiphase structures are distributed homogeneously.

As can be concluded from the microstructure analysis, the increase in the sintering temperature to 1200 °C for B and BT compacts results in the formation of densified and porous structures that are distributed homogeneously. The densified phase acts as a support for the porous structure and offers the suitable mechanical properties for the entire ceramic body used in the separation process. It follows from the SEM studies that valuable ceramic materials can be obtained from inexpensive waste material.

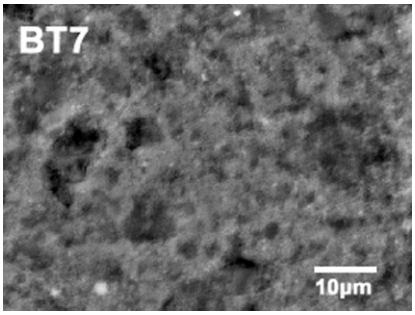

(a)

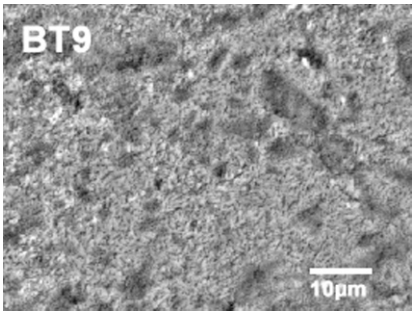

(b)

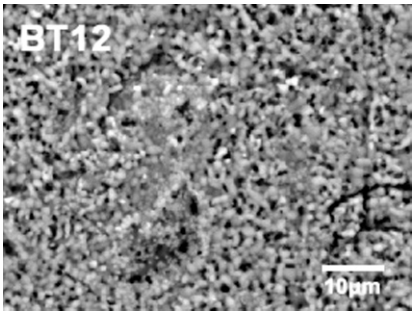

(c)

Fig. 5. SEM micrographs (magnification x = 1500) of BT compacts thermally treated for 1 h at (a) 700, (b) 900 and (c) 1200 °C.

3.6. Specific surface area measurements

Specific surface areas of the different samples are measured using N_2 gas as adsorbent. Prior to the analysis, the pressed samples are evacuated at 295 °C for 1 h. As given in Table 4, the increase in the values of specific surface area of B compacts with increasing the sintering temperature is caused by the microstructure variation and porous structure development as shown in Fig. 4(b–d).

In contrast, the decrease in the values of specific surface area of BT compacts with increasing the sintering temperature is caused by both the decrease in the average pore size in BT9 compact, compared to the BT7 one, and the increase in the average particle size in BT12 compact in comparison to the BT7 and BT9 ones, Fig. 5(a–c).

Table 4. Specific surface areas of the different sintered compacts.

	Specific surface area (m^2/g)		
Sample/Sintering temperature	700 °C	900 °C	1200 °C
B	45.0	86.5	121.7
BT	95.6	79.5	61.7

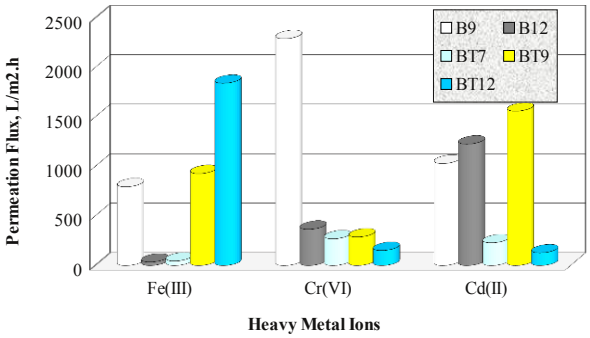

Fig. 6. Permeation fluxes through different membranes as a function of heavy metal ions.

3.7. Permeation study

B9, B12, BT7, BT9 and BT12 membranes are exposed to heavy metal ions in order to study the ions flow through these membranes and to identify the key parameters which control their transport through the membranes. As it is known, permeability is a property of membrane, which is independent of membrane thickness, and depends mainly on its microstructure and surface properties [19]. Pore size, surface roughness and surface charge of a membrane are studied as the key parameters for heavy metal ions transport. On this basis, a correlation of the permeate flux with the membrane structure is done, as given in Fig. 6. The initial fluxes of different heavy metal ions through different membranes are dependent on the structure of the membranes.

3.7.1. B membranes

The permeation fluxes of different heavy metal ions through B9 and B12 membranes are studied and given in Fig. 6. The remarkable decrease of both Fe(III) and Cr(VI) permeation fluxes through B12 membrane is caused by the decrease of the average pore size in B12 membrane in comparison to the B9 one, as shown in Fig. 4(d–c) respectively. Also the presence of large areas of densified matrix (β-TCP) can block and hinder the flow of the mentioned ions. On the other hand, the slight increase in Cd(II) permeation flux through B12 membrane indicates the existence of another factor, such as membrane roughness, dominating the transport of this ion through the selected membranes. A direct correlation exists between the decrease in membrane roughness and the transport of a particular ion through this membrane, as in the membranes with greater surface roughness, the deposition of ions or particles in the valleys of the rough membranes is increased, leading to the decrease in the permeation flux [20]. B12 membrane has smoother surface than the B9 one, as shown in Fig. 4(d–c) respectively, which overcomes the blocking and hindrance effect of the densified matrix in B12 membrane toward the transport of Cd(II) ion.

3.7.2. BT Membranes

The increase in Fe(III) permeation flux through the membranes, in the sequence: BT7, BT9 and BT12 (Fig. 6) is due to membrane surface roughness and membrane pore size variations, as shown in Fig. 5(a–c). It is concluded that the rougher surface of BT7 membrane retains certain ions as outlined above [20]. On the other hand, the decrease in the roughness of BT9 membrane and the increase of the average pore size of BT12 membrane are responsible for the increase in Fe(III) permeation flux through these membranes.

This result also explains the slight variations in Cr(VI) ions permeation flux for all tested BT membranes. The roughness of membrane surface has a big influence on the transport of Cd(II) ions through the BT membranes as follows from the large increase in permeation flux through BT9 membrane in comparison to BT7 one. The decrease of Cd(II) permeation flux through BT12 membrane may be due to membrane surface charge which in this case overcomes both the membrane pore size and membrane surface roughness effects, as the excess PO_4^{3-} ions at the surface creates negative charge [21]. In this case, the interactions between the membrane surface charge and the permeated ions affect the separation of certain ions regardless of membrane pore size distribution [22] as well as membrane surface roughness effects.

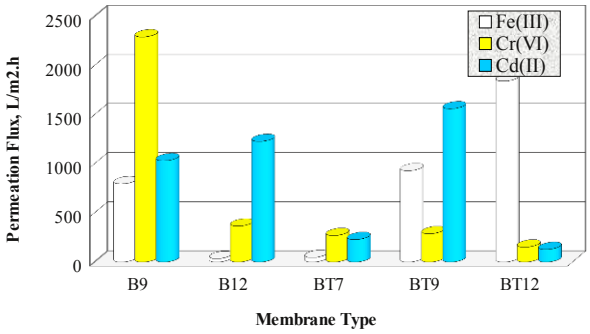

Fig. 7. Separation performance of the different studied membranes.

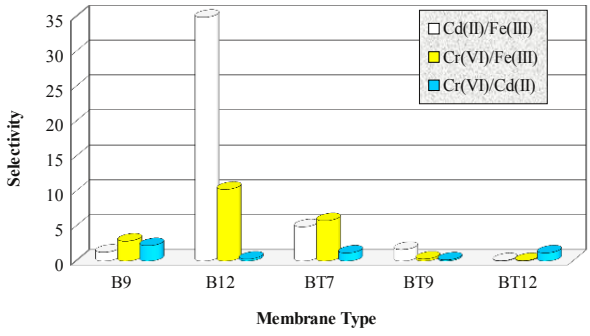

Fig. 8. Selective properties of the different studied membranes.

The differences in membrane structures between the different studied membranes lead to different selectivities under similar experimental conditions, as shown in Figs. 7–8. The membranes B9, B12 and BT7 (Fig. 7) are selective for Fe(III) ion separation from waste water solutions as follows from the lowest value of permeation flux in comparison to that of Cd(II) and Cr(VI) ions. In contrast, BT9 and BT12 membranes are selective for Cr(VI) and Cd(II) ions separation, respectively.

As can be concluded from Fig. 8, B12 membrane, due to its characteristic structure, is charac-

terized by the highest selectivity toward Cd(II) and Cr(VI) ions flow as compared to the other membranes. The densified phase acts as a blocker for the transport of certain ions with respect to others. On the other hand, when compared to other membranes, B9 membrane is characterized by the highest selectivity toward Cr(VI)/Cd(II). These conclusions follow from the permeation flux measurements and analysis of the factors that control the permeation or separation of certain ions as given before.

4. Conclusion

Meat bone wastes are considered as an inexpensive source of apatite-rich materials, mainly calcium hydroxyapatite (HAP, $(Ca_{10}(PO_4)_6(OH)_2)$ ceramics. The microstructure optimization is done by chemical and thermal treatments. The (HAP-TCP) composite materials are obtained by sintering at (700–1200) °C for 1 h. Furthermore, the addition of TiO_2 to pure bone material leads to the dissociation of the majority of HAP phase and the formation of perovskite ($CaTiO_3$), TCP ($Ca_3(PO_4)_2$) as well as rutile phases. The composite materials, fulfilling such requirements as high permeability, stability and mechanical strength, are prepared in the form of selective membranes. These membranes are used for heavy metal ions separation from waste water solutions. The transport of different heavy metal ions through the selected membranes is controlled by pore size, surface roughness and surface charge of the membranes. The dominating factor controlling this transport depends on membrane microstructure. It can be concluded that meat bone wastes can be treated and used as valuable ceramic materials to separate heavy metal ions from waste water solutions.

References

[1] MOHAMMADI T., RAZMI A., SADRZADEH M., *Desalination*, 167 (2004), 379.

[2] AJAYKUMAR A.V., DARWISH N.A., HILAL N., *World Applied Science J.* (Special Issue for Environmental), 5 (2009), 32.

[3] PAGANA A.E., SKLARI S.D., KIKKINIDES E.S., ZASPALIS V.T., *Microporous and Mesoporous Materials*, 110 (2008), 150.

[4] AL-ASHEH S., ABDEL-JABAR N., BANAT F., *Adv. Environ. Res.*, 6 (2002) 221.

[5] NAYAR S., GUHA A., *Mater. Sci. Eng. C*, 29 (2009), 1326.

[6] XIN F., JIAN CH., JIAN-PENG Z., QIAN W., ZHONG-CHENG Z., JIAN-MING R., *Trans. Nonferrous Met. Soc. China*, 19 (2009), 347.

[7] PRABAKARAN K., RAJESWARI S., *Trends Biomater. Artif. Organs*, 20 [1] (2006), 20.

[8] BALÁZSI C., WÉBER F., KÖVÉR, HORVÁTH E., NÉMETH C., *J. Eur. Ceram. Soc.*, 27 (2007), 1601.

[9] ZHU X., YANG W., *AIChE J.*, 54 [3] (2008), 665.

[10] IDRIS A., ZAIN N.M., *Journal Technology*, 44 [F] (2006), 27.

[11] KOZLOWSKI C., APOSTOLUK W., WALKOWIAK W., KITA A., *Problems of Mineral Processing*, 36, (2002), 115.

[12] ZHANG Y., CUI, H., OZAO R., CAO Y., CHEN B.I.T., WANG CH-W., PAN W-P., *Energy and Fuels*, 21 (2007), 3735.

[13] OZAWA M., SUZUKI S., *J. Am. Ceram. Soc.*, 85 [5] (2002), 1315.

[14] TADIC D., EPPLE M., *Biomaterials*, 25 (2004), 987.

[15] YOO D., KIM I., KIM S., HAHN CH.H., LEE CH., CHO S., *J. Non-Cryst. Solids*, 303 (2002), 134.

[16] CHOWDHURY, S.R., KUMAR P., BHATTACHARYA P.K., KUMAR A., *Separation and Purification Technology*, 24 (2001), 271.

[17] SANOSH K.P., CHU M-CH., BALAKRISHNAN A., KIM T.N., CHO S-J., *Curr. Appl. Phys.*, 10 (2010), 68.

[18] ERGUN C., DOREMUS R.H., *Turkish J. Eng. Env. Sci.*, 27 (2007), 423.

[19] LI L., DONG J., LEE R., *J. Colloid Interface Sci.*, 273 (2004), 540.

[20] JUNG JU LEE M.S. E.I., *Ph.D. thesis*, Ohio State University, Columbus, Ohio, USA (2009).

[21] VANDIVER J., DEAN D., PATEL N., BONFIELD W., ORTIZ CH., *Biomaterials*, 26 (2005), 271.

[22] ELIMELECH M., AMY G.L., CLARK M., *Am. Chem. Soc.*, 40 [2] (2000), 298.

Received 05-11-2011
Accepted 23-06-2012